Journal of Hazardous Materials 357 (2018) 10–18

Contents lists available at ScienceDirect

Journal of Hazardous Materials

journal homepage: www.elsevier.com/locate/jhazmat

Effect of surfactants on the interaction of phenol with laccase: Molecular docking and molecular dynamics simulation studies

Yujie Liu[a,b,1], Zhifeng Liu[a,b,1,*], Guangming Zeng[a,b,*], Ming Chen[a,b], Yilin Jiang[a,b], Binbin Shao[a,b], Zhigang Li[a,b], Yang Liu[a,b]

[a] College of Environmental Science and Engineering, Hunan University, Changsha, 410082, PR China
[b] Key Laboratory of Environmental Biology and Pollution Control, Hunan University, Ministry of Education, Changsha, 410082, PR China

GRAPHICAL ABSTRACT

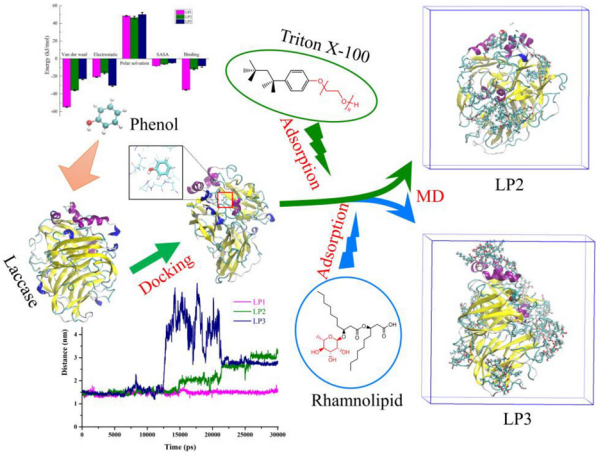

ARTICLE INFO

Keywords:
Laccase
Surfactants
Phenol
Enzymatic conformation
Biodegradation

ABSTRACT

Some surfactants can enhance the removal of phenol by laccase (Lac) in various industrial effluents. Their behavior and function in the biodegradation of phenolic wastewater have been experimentally reported by many researchers, but the underlying molecular mechanism is still unclear. Therefore, the interaction mechanisms of phenol with Lac from *Trametes versicolor* were investigated in the presence or absence of Triton X-100 (TX100) or rhamnolipid (RL) by molecular docking and molecular dynamics (MD) simulations. The results indicate that phenol contacts with an active site of Lac by hydrogen bonds (HBs) and van der Waals (vdW) interactions in aqueous solution for maintaining its stability. The presence of TX100 or RL results in the significant changes of enzymatic conformations. Meanwhile, the hydrophobic parts of surfactants contact with the outside surface of Lac. These changes lead to the decrease of binding energy between phenol and Lac. The migration behavior of water molecules within hydration shell is also inevitably affected. Therefore, the amphipathic TX100 or RL may influence the phenol degradation ability of Lac by modulating their interactions and water environment. This study offers molecular level of understanding on the function of surfactants in biosystem.

* Corresponding authors at: College of Environmental Science and Engineering, Hunan University, Changsha, 410082, PR China.
E-mail addresses: zhifengliu@hnu.edu.cn (Z. Liu), zgming@hnu.edu.cn (G. Zeng).
[1] These authors contribute equally to this article.

https://doi.org/10.1016/j.jhazmat.2018.05.042
Received 6 December 2017; Received in revised form 1 May 2018; Accepted 21 May 2018
Available online 22 May 2018

1. Introduction

Phenol and its chemical derivatives are commonly used for raw materials in many industrial fields, for instance, tannery, petrochemical, paper, chemical and pharmaceutical industries [1]. Excessive discharge of phenolic wastewater into natural environment causes severe water pollution, and further threaten human health even at a very low concentration [2]. The concentration of phenolic compounds has exceeded 1.0 mg/L in various industrial wastewater, thus it is hard to reduce it up to the specified concentration (0.1–1.0 mg/L) due to its solubility and stability in water [3]. Phenol and its vapors can harm the skin, respiratory tract, and the eyes, and seriously can cause acute toxicity with mutagenic and carcinogenic characters [4]. At present, many conventional methods have been used for treating phenol-containing wastewater, such as chemical oxidation, physical absorption, photocatalysis, solvent extraction and biodegradation [1,2]. As shown in Table S1, every method is not perfect because of its double sides. With more attention paid to the environmental protection and sustainable development, plenty of researchers are more concerned about biodegradation of phenol due to its outstanding capacity of decomposition and low secondary pollution [5]. Although many factors still restrict the removal efficiency of phenol, including the degradation capacity of microorganisms, enzymatic activity and the environmental factors (e.g., temperature, oxygen, water, and pH) [5,6], biological treatment is a crucial part in many sewage treatment plants. In the stage of biodegradation, various enzymes secreted by microorganisms are responsible for the transformation and decomposition of contaminants. Laccases are mainly isolated from plants and fungus [7]. It belongs to oxidoreductase with high redox potential. They are extensively implemented to eliminate phenols in wastewater treatment during the past few of years [8,9]. However, the removal efficiency of phenols by laccase (Lac) in the absence of other additives is undesirable due to the hydrophobicity and toxicity of phenols [10,11].

For hydrophobic organic compounds (HOCs), many surfactants could significantly enhance their removal efficiencies [12–14]. Surfactants are classified as two main types according to the sources, including chemical surfactants and biosurfactants [12]. The former is often synthesized by chemical industries, while the latter is generally produced via specific microorganisms or plants under certain conditions. For example, synthetic surfactants typically include sodium dodecyl sulfate, Triton X-100, cetyl trimethyl ammonium bromide, Brij35, etc. [13]. In addition, there are two different biosurfactants, including microbial-based and plant-based surfactants. The microbial-based biosurfactants, such as glycolipids, phospholipids, and lipopeptides, are usually produced by *Pseudomonas spp., Candida spp.,* etc. [15]. On the other hand, the plant-based surfactants (eg., sapindus mukurossi and saponin) are extracted from sapindus and genus Camellia [13,16]. They are widely employed to manufacture detergent for our daily life, as emulgator for pesticides, making sanitizer for pharmaceutical industry, and increasing solubility of organic matters in aqueous phase [13,17]. Until now, enormous attention is paid to the widespread use of surfactants to improve the biodegradation ability of various organic pollution because they could increase the bioavailability of HOCs and influence cell surface properties of microorganisms [11,18–24]. Mao et al. [25] summarized the application of various surfactants on the remediation of polluted soils, it showed that the solubilizing capability, adsorption behavior and biocompatibility of surfactants play an essential role in the removal of HOCs, heavy metals and radionuclides. Numerous studies also indicated that the addition of specific surfactants (e.g., Triton X-100, rhamnolipid, Tween 80) during the biodegradation of phenols with laccases could obviously increase their removal efficiencies by protecting the enzyme from the poisonousness of phenols, changing enzyme's activity sites, and availably enhancing the solubility of phenols to contact with enzyme, etc. [9,10,26,27]. However, in these previous studies, it was lack of investigation on the influence of surfactants/biosurfactants on the interaction and removal process of phenols with Lac at molecular level.

This motivates the present work, in which we study the interaction of phenol with Lac in the coexistence of Triton X-100 (TX100) or rhamnolipid (RL). By means of molecular docking and molecular dynamics (MD) simulation, the behavior of Lac, phenol and surfactants is revealed in aqueous systems. Herein, this work mainly investigates the effects of the two surfactants on the entire stability of Lac, conformational transformation of complexes, hydrogen bonds, binding energy distribution, and dynamic transformation of water molecules during the biodegradation of phenol by laccase-oxidation. These outcomes would be useful to provide theoretical knowledge about the biodegradation phenomena of phenol.

2. Theoretical background and computational details

2.1. Theoretical background

2.1.1. Reliability of initial binding matrix

The initial binding matrix was proposed by carrying out Molegro Virtual Docker (MVD) [28]. MVD used the docking search algorithm based on evolutionary algorithm to find the lowest energy region of Lac and put phenol molecule into this area. According to the related report, the accuracy of MVD is 87%, which universally exceeds other molecular docking software [29]. Therefore, we think that the binding model given by MVD is reliable.

2.1.2. The motion of particles

MD simulations describe the physical movements of particles by solving Newton's equations for a system of N interacting particles:

$$m_i \frac{\partial^2 r_i}{\partial t^2} = F_i,\ i = 1,\ \ldots, N$$

For particle i, the mass is m_i, the displacement within time interval (t) is r_i, the force is F_i.

The interactions of particles depend on coulomb forces and other non-bonded interactions. In this study, we calculated the atomic charge of phenol and surfactants at the B3LYP/6-31G* level based on Automated Topology Builder website [30]. The charge distribution of Lac was given from GROMOS 54a7 force field [31] in Gromacs package [32]. The coulomb forces are confirmed by coulomb's law, while other non-bonded forces are also described by Lennard-Jones potential [33]. The Lennard-Jones potential of particle i and j ($V_{LJ}(r_{ij})$) can be computed by the below equation:

$$V_{LJ}(r_{ij}) = 4\varepsilon_{ij}\left(\left(\frac{\sigma_{ij}}{r_{ij}}\right)^{12} - \left(\frac{\sigma_{ij}}{r_{ij}}\right)^{6}\right)$$

Where ε_{ij} is the depth of the potential well, r_{ij} represents the distance between the particles, and σ_{ij} is the distance at which the inter-particle potential is zero.

2.1.3. Calculation of binding energy

Binding energy was defined as [34],

$$G_{binding} = G_{complex} - G_{free\text{-}protein} - G_{free\text{-}ligand}$$

$G_{binding}$ is binding free-energy, $G_{complex}$ is the total energy of complex, and the $G_{free\text{-}protein}/G_{free\text{-}ligand}$ is total free energies of the isolated protein and ligand in solvent, respectively. The g_mmpbsa [34] tool was employed to calculate energy distribution in this study. Solvent accessible surface area (SASA) model was used to compute nonpolar energy relying on the following equation with high accuracy [35],

$$G_{nonpolar} = \gamma A + b$$

Where $G_{nonpolar}$ is the non-electrostatic contributions to the solvation free energy, γ is a coefficient for surface tension of the solvent, A and b are SASA and fitting parameter, respectively.

Table 1
The physicochemical properties of phenol and the surfactants.

Full name	Chemical formula	Abbreviation	Molecular weight/(g/mol)	Water solubility/(g/100 mL)	CMC/(μM)
Phenol	C_6H_5OH	Phenol	94.11	8.3	–
Triton X-100	$C_{14}H_{21}(C_2H_4O)nOH$	TX100	646.85	soluble	220 ~ 240
Mono-rhamnolipid	$C_{26}H_{48}O_9$	RL	504.65	soluble	10 ~ 120

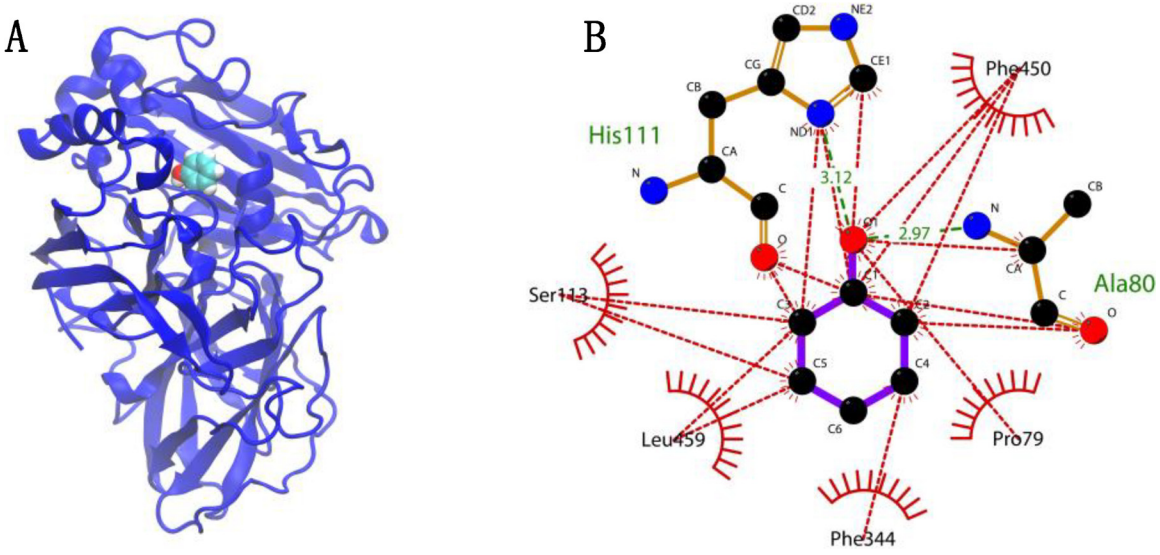

Fig. 1. The initial structures of Lac and phenol and their interactions.
(A) The backbone of Lac was shown as blue strip, while the cyan, red and white represented C, O and H atoms of phenol, respectively; (B) The interactions between Lac and phenol. Hydrogen bonds were shown as green dotted lines, while the spoked arcs represented residues of Lac making non-bonded contacting with phenol, and red dotted lines also described the hydrophobic interactions among their atoms in detail. (For interpretation of the references to colour in this figure legend, the reader is referred to the web version of this article).

2.2. Computational details

2.2.1. Construction of computational systems

In this study, phenol was implemented to act as a typical organic pollutant and two surfactants including TX100 and RL were employed as solute molecules during the simulation. The reliable 3D structure of Lac (PDB ID: 1GYC) reported in white-rot fungus was obtained from RCSB website (http://www.rcsb.org/pdb/home/home.do). The information on their water solubility, molecular weight, and critical micelle concentration (CMC) derived from previous investigations [23,36,37] were given in Table 1. Their 2D structures were also exhibited in Fig. S1. MD simulations were utilized for studying the dynamics of binary systems with the coexistence of Lac and phenol (LP1) and ternary systems with Lac, phenol and TX100 (LP2) or RL (LP3). Other six systems acted as comparison groups, including the system with the presence of only Lac (Lac(aq)) or phenol (Phenol(aq)), the copresence of Lac and TX100 (LT) or RL (LR), the incorporation of phenol and TX100 (PT) or RL (PR). Therefore, a total of nine systems were constructed in the present study, and more details were shown in Table S2. The number of TX100 or RL molecules was 23 for performing the better behavior of aggregation[38] in every system with surfactants.

2.2.2. Computational parameter

Firstly, initial binding matrix was obtained by MVD. In the case, grid resolution of MolDock Score was set at 0.30 Å with 1500 of max iteration and 0.50 Å resolution of predicting the binding cavity of Lac for gaining the best result. In addition, original ligands of Lac were removed manually before running docking [39]. Docking process was carried out five times to avoid an accidental error. The complex of the best reranking score was selected for further research from many possible structures.

Subsequently, Gromacs (v5.1.4) simulation package was employed in present study to simulate all reaction systems, which belongs to an open source MD software with high efficiency by GPU acceleration [32,40]. All simulations used GROMOS 54a7 force field [31] due to its compatibility and stability for systems of biomacromolecule with organic molecules [39]. All systems were set in the same conditions as 298 K of temperature, 8 nm × 8 nm × 8 nm of cubic box, and Simple Point Charge (SPC) water model [41] for their comparison. Moreover, the short-range electrostatic cut-off was 1.4 nm and using Particle Mesh Ewald (PME) [42] for long-range electrostatics in order to gain the best consequence. For each system, 200 ps canonical ensemble (NVT) + 200 ps isothermal-isobaric ensemble (NPT) + 30 ns MD simulations were executed under the periodic boundary condition. Another input parameters for g_mmpbsa such as solute dielectric constant, solvent dielectric constant, and solvent probe radius were set as 2, 80, and 1.4 Å for obtaining the best result [34], respectively.

2.2.3. Analysis of MD trajectory

The trajectory of MD simulation was extracted for LP1, LP2 and LP3 systems and saved at interval 100 ps for free energy calculation in the last 10 ns. The total of 202 frames was used to calculate binding free energy eventually. The number of water molecules within 5 Å of phenol was calculated by a Tool Command Language script from Visual Molecular Dynamics (VMD) software [49] in this investigation.

3. Results and discussion

3.1. Conformations

3.1.1. Structure profiles and interactions of initial Lac with phenol

Fig. 1A represented the optimal complex of Lac and phenol, the

phenol molecule was trapped into a special cavity of Lac. The optimal complex was confirmed by comparing the MolDock score, Rerank score and binding affinity from MVD, their values were −52.467, −47.793 and −60.085 kJ/mol, respectively. Furthermore, we also determined some interactions of Lac and phenol via LigPlot$^+$ [43], and the two-dimension diagram was shown in Fig. 1B. Xu et al. [44] found hydroxyl group of phenolic compounds makes it easier to be oxidized by fungal Lac via one-electron reaction yielding free radical than other substituents (e.g., $-NO_2$ and $-COCH_3$). We also found the existence of hydrogen bonds between the oxygen atom of phenol and nitrogen atoms of His111/Ala80 (abbreviation of amino acid plus its number, the same as below), the bond lengths were 3.12 Å and 2.97 Å, respectively. In addition, Ser113, Leu459, Phe344, Pro79, and Phe450 as hydrophobic groups affected the combination and stability of the complex of Lac and phenol. This result was in agreement with the interactions between Lac and nonylphenol/octylphenols reported by Mo et al. [45], both phenolic compounds were bound to the same active site of Lac with some common residues, such as Phe344, Phe450 and Leu459. Therefore, hydrogen-bond interactions, together with hydrophobic contacts, were necessary to the interactions of phenolic pollutants with Lac. The viewpoint was also testified by Chen's investigation on molecular basis of Lac bound to lignin model compounds [39].

3.1.2. Conformational transformation during MD simulation

The related literature [46] reported that the surfactant led to conformational changes of enzyme by interacting with the enzyme. In this study, we also observed the structural changes of Lac-phenol complex in the presence of TX-100 or RL in Fig. 2. The surfactants spontaneously aggregated into many conformations each other around the surface of Lac at 10 ns in LP2 and LP3, which affected the structure of Lac and resulted in the decrease of enzyme surface contacted with liquid. Lou et al. [47] also proposed a protecting mechanism that some non-ionic surfactants could reduce enzyme deactivation caused by adverse environment such as air-liquid interface and mechanical agitation. However, the conformation of Lac-phenol complex in LP1 didn't change obviously at different time points, while the orientation of phenol turned slightly. It implied that the Lac-phenol complex was steady in the bulk water [39]. Another phenomenon was that the distance of center of mass (COM) among Lac-phenol without surfactants retained the constant of 1.5 nm (Fig. S2). Therefore, the binding model of Lac with phenol for its biodegradation based on the docking result of MVD was acceptable. The tremendous changes of COM (Fig. S2) occurred within the range from 12 ns to 22 ns in LP2 and LP3, which suggested that the presence of surfactants had a great influence on its binding status. The calculation of root-mean-square deviation (RMSD) was shown in Fig. 3A. The RMSD values increased rapidly at the first 10 ns and then reached steady at 30 ns, which showed that the structures were transformed for novel environment. The equilibrium value of RMSD was about 2.5 Å in LP1. The result was in accordance with the findings reported by Chen et al. [39]. The significance analysis of RMSD with or without surfactants reported that significant difference was caused by the addition of surfactants ($t = 29.724$, $p < 0.01$ for Lac(aq) and LT; $t = 30.081$, $p < 0.01$ for Lac(aq) and LR; $t = 90.033$, $p < 0.01$ for LP1 and LP2; $t = -21.436$, $p < 0.01$ for LP1 and LP3). In view of the folding of Lac (Fig. 3B), the radius of gyration (Rg) value decreased in LP1 while it mildly increased in LP2 and LP3. It was also seen that Rg of Lac in LP2 showed less fluctuation than that of LP3 due to its interactions with different surfactants [27]. Additionally, the Rg values of phenol (Table S3, Fig. S3) maintained stable in Phenol(aq), PT and PR systems, which were attributed to its simple structure and

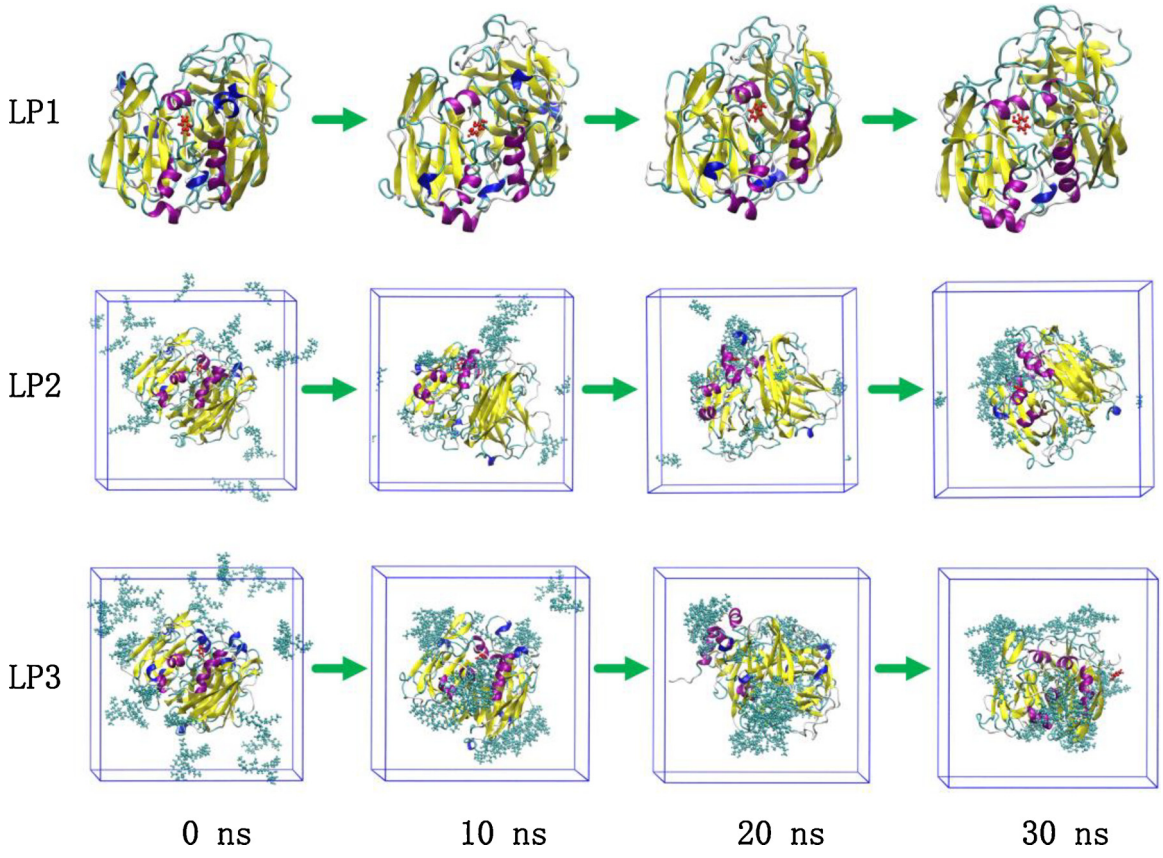

Fig. 2. Conformational transformation of complexes in the model system LPn (n = 1, 2, 3).
The red cyclic structure represented phenol and the cyan ball-and-stick configuration was TX100 or RL. The secondary structure of Lac was also exhibited in cartoon pattern. Note, the water molecules were not shown for simplicity. (For interpretation of the references to colour in this figure legend, the reader is referred to the web version of this article).

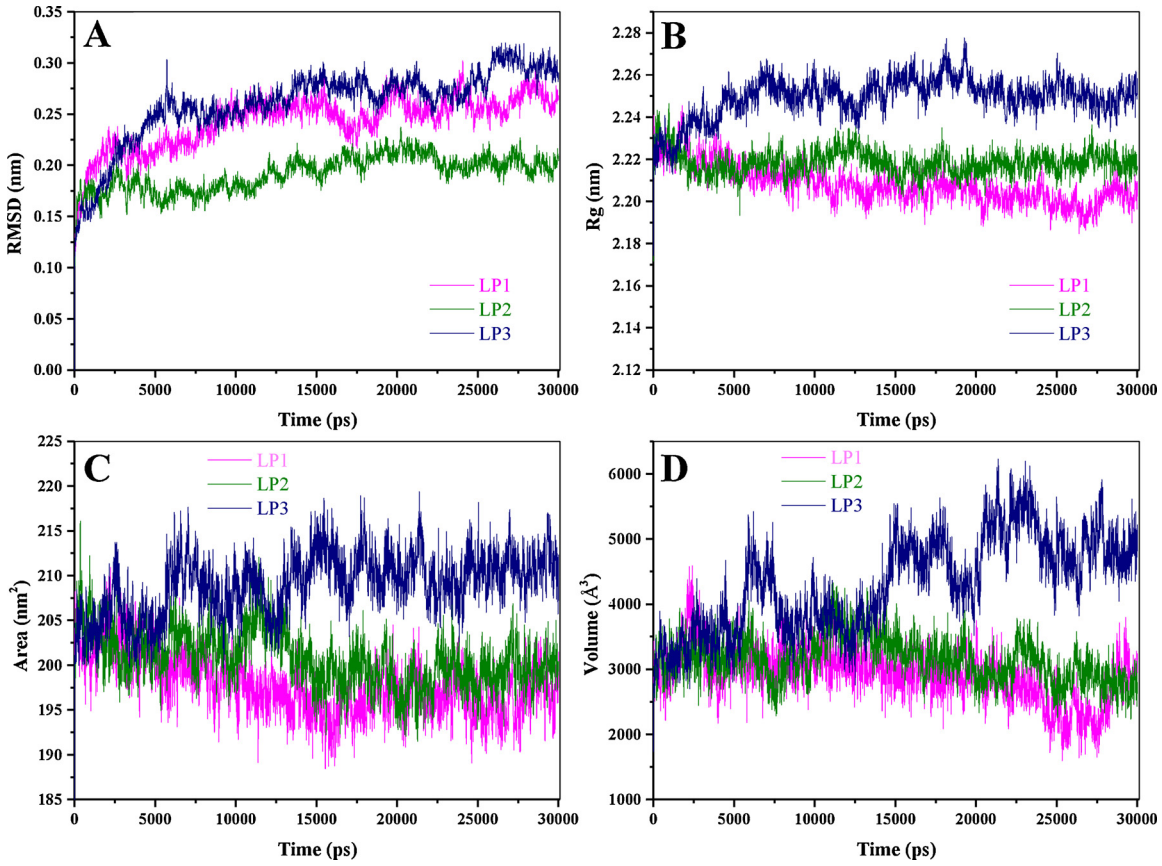

Fig. 3. The variation of (A) root-mean-square-deviations (RMSD), (B) radius of gyration (Rg), (C) solvent accessible surface area (SASA) and (D) volume of cavities (Vc) in LPn (n = 1, 2, 3).

rigidity of benzene ring. In addition to these above results, the overall folding of amino acids of Lac in LP1 and LP2 was accompanied by a reduction of its solvent accessible surface area (SASA) [48] in Fig. 3C. For Lac, it had the largest SASA value in its stretched conformation. The SASA values of LP2 and LP3 systems were higher than that of LP1 system. Therefore, the amino acids from Lac unfolded its compact structure in the presence of surfactants, some water molecules around the surface of Lac could be driven into newly opened pocket. These water solvent molecules closed pockets may be hydration shell water. Previous study also indicated that the cavities and channels of protein play an essential role in studying protein-ligand binding, molecular transport, and enzyme catalysis [49]. In present study, the volume of cavities (Vc) [50] value of Lac in LP3 was bigger than that of in LP1 or LP2 (see Fig. 3D). This indicated that more cavities were formed on the surface of Lac. The addition of RL molecules changed local topology of Lac surface other than bulk water environment. More importantly, the cavities variation would interfere with the enzyme-catalyzed process [51].

The above analysis demonstrated that Lac and surfactants formed complex clusters spontaneously in aqueous solution [52], driven by their electrostatic interactions in GROMOS 54a7 force filed. Lac unfolded its amino acids of surface binding with surfactants, which affected the behavior of phenol. The binding site of phenol moved to another pocket of Lac in order to adapt this change. These results showed that TX100 and RL may influence folding behavior of Lac and interactions between Lac and phenol through dissimilar methods [21]: (1) Majority of TX100 and RL improved the unfolding of Lac by electrostatic force; (2) Some surfactants molecules directly interacted with phenol by vdW and electrostatic interactions. These findings can reasonably explain the behavior of surfactants reported by experimental investigation.

3.2. Interaction mechanism between Lac and phenol in different systems

3.2.1. Hydrogen bonds (HBs) dynamics

It was commonly known that HBs were of great importance for protein-ligand interaction, stability of biomacromolecule, and enzymatic catalysis [53,54]. The HBs dynamics of Lac-phenol complexes with or without surfactants were shown in Fig. 4. The presence of surfactants (TX100 or RL) changed the HBs between Lac and phenol. The phenol mainly formed two kinds of HBs (see Table 2) in the whole simulation: one was composed of hydroxyl oxygen of phenol with nitrogen atoms of Lac, another consisted of hydroxyl oxygen of phenol with water molecules. In addition, TX100 or RL distinctly increased the number of HBs between phenol and water after 7 ns as shown in Fig. S4. These HBs might disturb the formation of HBs between Lac and phenol. Previous investigation also reported that the surfactant could form hydrogen bonds with phenolic groups of degrading enzyme, which prevented enzyme-substrate adsorption [55].

3.2.2. Dynamic distribution of interaction energies

The interaction energies between Lac and phenol at the last 10 ns were plotted in Fig. S5. In these three systems, both electrostatic and vdW interactions (always negative value of energies) favored the binding of phenol to Lac. The electrostatic interactions in LP2 were frequently fluctuated in the equilibrium position of LP1, while this interaction in LP3 was obviously lower than that of LP1 system. The vdW interactions in LP2 and LP3 showed much more fluctuation than that in LP1, suggesting the binding model between Lac and phenol suffered more changes on account of the binding of surfactants to Lac or phenol. This was similar to the case of Rg and SASA in previous description, indicating that the presence of surfactants resulted in the following outcomes: (1) To a certain extent, it facilitated the unfolding of Lac,

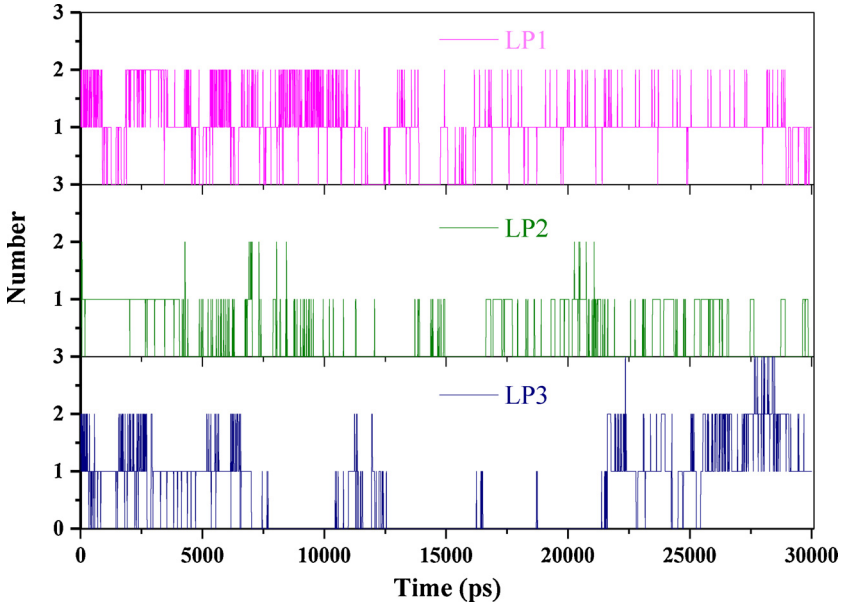

Fig. 4. Hydrogen bonds between Lac and phenol in LPn (n = 1, 2, 3).

which indirectly weakened the vdW interactions between Lac and phenol; (2) Some TX100 or RL molecules migrated to around the phenol, this phenomenon interfered the electrostatic interactions of Lac-phenol complex. The accurate calculation of binding free-energy was one of the most important works for researching biochemical reaction. The MM/PBSA method was widely used to calculate the binding energy in many research fields [54,56,57]. In our study, binding free energies were computed by this method. As shown in Fig. 5A, the addition of TX100 or RL significantly reduced the binding stability of phenol. The changes of vdW interactions were consistent with the binding energy. Therefore, vdW interactions played a dominant role in the stability of complex. In previous study, the vdW interactions were the primary force that facilitated the lignin model compounds to the Lac from plant and fungus [58]. Another interesting finding was that the polar solvation energy and SASA energy changed a little with or without surfactants. This suggested that the solvent environment in different systems for the changes of binding energy gave poor contributions. In addition, the electrostatic energy between phenol and Lac in LP3 was prominently lower than that of LP1 and LP2 systems. The difference of electrostatic energy may be attributed to the charge property of surfactants, since TX100 belongs to non-ionic surfactants while RL is with negative charge in aqueous solution.

Contribution energy of each residue to total binding energy was shown in Fig. 5B. The results showed that three residues (Leu459, Phe81 and Glu460) mainly provided the binding region with large energy (absolute value was larger than 2 kJ/mol) in LP1, while there was only one residue (Asp492) in LP2 and two residues (Asp50, Lys59) in LP3, respectively. For quantitative analysis of the key residues, the following formula according to a previous work [54] with modification was used:

$$K_D = \begin{cases} 1, & D \geq 1.5\ \text{kJ/mol} \\ 0, & D < 1.5\ \text{kJ/mol} \end{cases}$$

$$D = |G_0 - G_i|$$

Where K_D is the abbreviation of key residues; G_0 is the binding energy of each residue in the absence of surfactants. G_1 and G_2 (G_i), are the binding energy of each residue in the presence of TX100 and RL, respectively. In addition, the value "1" of K_D indicates that the residue is key residue.

There were five key residues (Asp492, Leu459, Phe81, Glu460, and Gln499) between Lac and phenol in the presence of TX100, and seven key residues (Asp50, Leu459, Phe81, Glu460, Lys59, Pro346 and Thr51) in the presence of RL. These residues of Lac had a major impact on the changes of binding energy. Previous review [49] also summarized the function of amino acids in enzyme catalysis. It indicated that some charged residues, such as Glu, Asp, Arg, and Lys, were implemented to provide charges that influenced the substrate and other residues in the course of biodegradation. In above analysis, those key residues also may affect the catalytic ability of Lac to phenol.

3.3. Dynamic transformation of water molecules

3.3.1. Water molecules overlapping Lac cavities

The amount of water molecules overlaying the surface of Lac cavities (abbreviate as N_W) was counted by trj_cavity [50] as shown in Fig. 6A. The N_W values kept around 300 in LP1 as well as that in LP2, but more fluctuation appeared in LP3. This meant that RL would mightily modulate the posture and folding of Lac. A recent paper [59] also detailedly discussed the mechanism of formation of surfactant/

Table 2
The form of HBs between phenol and other components in several typical simulation time.

Time/(ns)	LP1		LP2		LP3	
	Number	Type	Number	Type	Number	Type
0	2	HO-N(His111,Ala80)	1	HO-N(His111)	2	HO-N(His111,Ala80)
10	1	HO-OW	2	HO-OW	2	HO-OW
20	1	HO-OW	1	HO-OW	2	HO-OW
30	0	–	3	HO-OW	2	HO-OW

HO represented the hydroxyl of phenol, N was the nitrogen atom of residues of Lac, and OW was oxygen atom of water molecule.

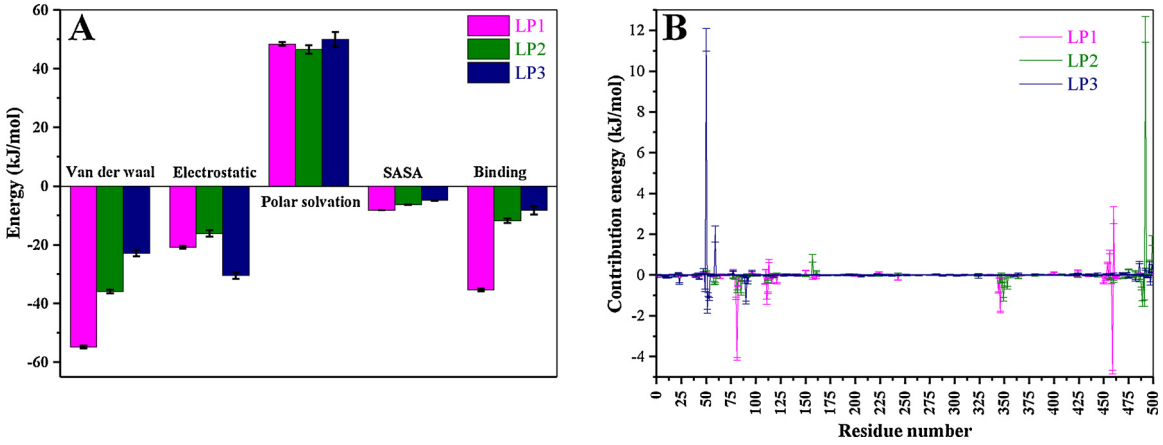

Fig. 5. Energy contribution of Lac-phenol complex in LPn (n = 1, 2, 3).
(A) the different types of energy; (B) contribution energy of each residue.

protein adsorption layers, it emphasized that ionic surfactants were easier to absorb on the surface of protein than non-ionic types due to the high affinity. Consequently, RL at a high concentration could cause gradual denaturation of the protein, corresponding to the unfolding of Lac in this investigation.

3.3.2. The number of water molecules in binding region of Lac and phenol

The water molecules were divided into hydration shell water and bulk water, the former was defined by a 4.9 Å distance restriction between the non-hydrogen atoms of phenol or Lac and water oxygen atoms, while this distance of bulk water was larger than 4.9 Å [60]. The density of water on the surface of enzyme was markedly higher than that of bulk water, which could affect the hydrophilicity/hydrophobicity of the surface of molecules [61,62]. In previous studies, water molecules within 5 Å of binding region played a significant role in the process of biodegradation [51,54]. Based on the findings of prior research [51,63], the water molecules around the binding region were likely to promote or inhibit biochemical reaction in biodegradation. Accordingly, the number of water molecules within 5 Å of phenol (abbreviate as N_P) was shown in Fig. 6B. These curves represented the fluctuation of N_P over simulation time and indicated their own solvent environment. The initial N_P in LP3 was about 5 as well as that in LP1. The value gradually rose at 5 ns until up to the maximum of ~40 from 13 ns to 22 ns, and then decreased slowly and finally achieved new stability. Furthermore, similar phenomena were observed in LP2, its peak of N_P (about 25) was smaller than that of LP3. This variation might be caused by different ways: (1) surfactants closed to phenol, it occupied those interspace combined with solvent in vicinity of phenol; (2) the unfolding of amino acid chains in binding region of Lac-phenol released more extra space led to the access of bulk water molecules; (3) the presence of surfactants altered the distribution of electrostatic force [21], it affected the interactions between phenol and water molecules within 5 Å distance.

4. Conclusions

In conclusion, the molecular interactions of Lac and phenol were studied in the presence or absence of surfactants at molecular level in this study. The results indicated that surfactants could change the conformations of Lac and the interactions between Lac and phenol. The anionic surfactant RL was stronger than nonionic surfactant TX-100 on leading to unfolding of Lac. The primary driving force for the binding between Lac and phenol was vdW interactions, which was agree with previous research. Moreover, the present study also found that the HBs and water behavior between Lac and phenol were affected by the addition of surfactants. This study contributes to understanding the relationship of surfactants and Lac. It will be significant for future research to look for a great additive in order to improve enzyme reaction.

Acknowledgments

The study was financially supported by the Program for Changjiang Scholars and Innovative Research Team in University (IRT-13R17), the National Natural Science Foundation of China (51679085, 51378192,

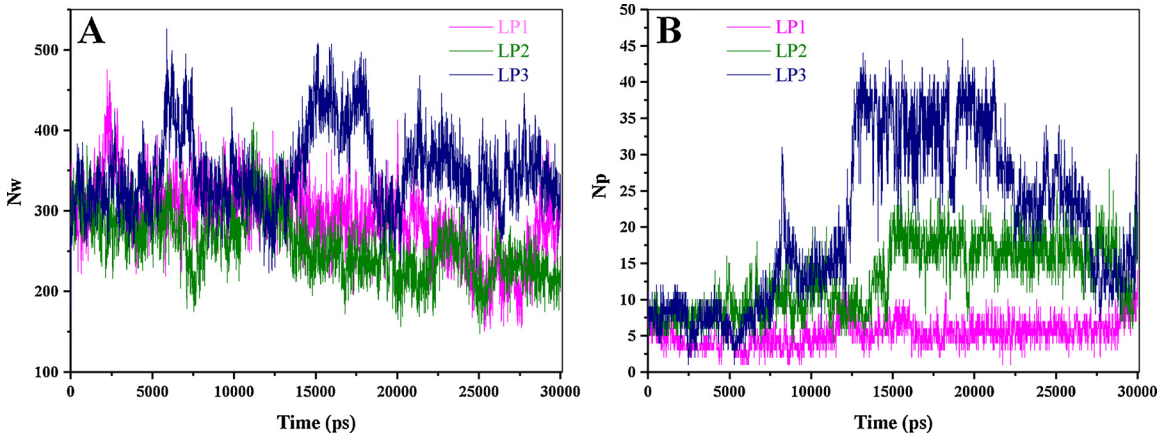

Fig. 6. Time evolution of water molecules in LPn (n = 1, 2, 3).
(A) The number of water overlapping Lac cavities; (B) The number of water molecules within 5 Å of phenol.

51039001, 51378190, 51521006, 51508177), the Fundamental Research Funds for the Central Universities of China (531107050930), Hunan Provincial Innovation Foundation for Postgraduate (CX2017B098).

Appendix A. Supplementary data

Supplementary material related to this article can be found, in the online version, at doi:https://doi.org/10.1016/j.jhazmat.2018.05.042.

References

[1] L.F. Ren, R. Chen, X. Zhang, J. Shao, Y. He, Phenol biodegradation and microbial community dynamics in extractive membrane bioreactor (EMBR) for phenol-laden saline wastewater, Bioresour. Technol. 244 (2017) 1121–1128.
[2] G. Pan, K.I. Kurumada, Hybrid gel reinforced with coating layer for removal of phenol from aqueous solution, Chem. Eng. J. 138 (2008) 194–199.
[3] V. Vaiano, M. Matarangolo, J.J. Murcia, H. Rojas, J.A. Navío, M.C. Hidalgo, Enhanced photocatalytic removal of phenol from aqueous solutions using ZnO modified with Ag, Appl. Catal. B: Environ. 225 (2018) 197–206.
[4] A. Turki, C. Guillard, F. Dappozze, Z. Ksibi, G. Berhault, H. Kochkar, Phenol photocatalytic degradation over anisotropic TiO2 nanomaterials: kinetic study, adsorption isotherms and formal mechanisms, Appl. Catal. B: Environ. 163 (2015) 404–414.
[5] N.V. Pradeep, S. Anupama, K. Navya, H.N. Shalini, M. Idris, U.S. Hampannavar, Biological removal of phenol from wastewaters: a mini review, Appl. Water Sci. 5 (2014) 105–112.
[6] C.I. Nair, K. Jayachandran, S. Shashidhar, Biodegradation of phenol, Afr. J. Biotechnol. 7 (2008) 4951–4958.
[7] D.L. Huang, G.M. Zeng, C.L. Feng, S. Hu, X.Y. Jiang, L. Tang, F.F. Su, Y. Zhang, W. Zeng, H.L. Liu, Degradation of lead-contaminated lignocellulosic waste by phanerochaete chrysosporium and the reduction of lead toxicity, Environ. Sci. Technol. 42 (2008) 4946–4951.
[8] B. Uhnakova, A. Petrickova, D. Biedermann, L. Homolka, V. Vejvoda, P. Bednar, B. Papouskova, M. Sulc, L. Martinkova, Biodegradation of brominated aromatics by cultures and laccase of trametes versicolor, Chemosphere 76 (2009) 826–832.
[9] Z. Asadgol, H. Forootanfar, S. Rezaei, A.H. Mahvi, M.A. Faramarzi, Removal of phenol and bisphenol-A catalyzed by laccase in aqueous solution, J. Environ. Health Sci. Eng. 12 (2014) 1–5.
[10] Z.F. Liu, G.M. Zeng, H. Zhong, X.Z. Yuan, H.Y. Fu, M.F. Zhou, X.L. Ma, H. Li, J.B. Li, Effect of dirhamnolipid on the removal of phenol catalyzed by laccase in aqueous solution, World J. Microbiol. Biotechnol. 28 (2012) 175–181.
[11] F. Li, L. Zhu, L. Wang, Y. Zhan, Gene expression of an arthrobacter in surfactant-enhanced biodegradation of a hydrophobic organic compound, Environ. Sci. Technol. 49 (2015) 3698–3704.
[12] S. Paria, Surfactant-enhanced remediation of organic contaminated soil and water, Adv. Colloid Interface Sci. 138 (2008) 24–58.
[13] S. Lamichhane, K.C. Bal Krishna, R. Sarukkalige, Surfactant-enhanced remediation of polycyclic aromatic hydrocarbons: a review, J. Environ. Manage. 199 (2017) 46–61.
[14] Y. Liu, G. Zeng, H. Zhong, Z. Wang, Z. Liu, M. Cheng, G. Liu, X. Yang, S. Liu, Effect of rhamnolipid solubilization on hexadecane bioavailability: enhancement or reduction? J. Hazard. Mater. 322 (2017) 394–401.
[15] S. Vijayakuma, V. Saravanan, Biosurfactants-types, sources and applications, Res. J. Microbiol. 10 (2015) 181–192.
[16] N. Guo, T. Tong, N. Ren, Y. Tu, B. Li, Saponins from seeds of genus Camellia: phytochemistry and bioactivity, Phytochemistry 149 (2018) 42–55.
[17] J. Wei, G. Huang, C. An, H. Yu, Investigation on the solubilization of polycyclic aromatic hydrocarbons in the presence of single and mixed gemini surfactants, J. Hazard. Mater. 190 (2011) 840–847.
[18] T.L. Cort, M.S. Song, A.R. Bielefeldt, Nonionic surfactant effects on pentachlorophenol biodegradation, Water Res. 36 (2002) 1253–1261.
[19] P.K. Mohan, G. Nakhla, E.K. Yanful, Biokinetics of biodegradation of surfactants under aerobic, anoxic and anaerobic conditions, Water Res. 40 (2006) 533–540.
[20] M. Bueno-Montes, D. Springael, J.J. Ortega-Calvo, Effect of a nonionic surfactant on biodegradation of slowly desorbing PAHs in contaminated soils, Environ. Sci. Technol. 45 (2011) 3019–3026.
[21] M. Goldfeder, A. Fishman, Modulating enzyme activity using ionic liquids or surfactants, Appl. Microbiol. Biotechnol. 98 (2014) 545–554.
[22] Z.F. Liu, G.M. Zeng, H. Zhong, X.Z. Yuan, L.L. Jiang, H.Y. Fu, X.L. Ma, J.C. Zhang, Effect of saponins on cell surface properties of Penicillium simplicissimum: performance on adsorption of cadmium(II), Colloids Surf. B. Biointerfaces 86 (2011) 364–369.
[23] B. Shao, Z. Liu, H. Zhong, G. Zeng, G. Liu, M. Yu, Y. Liu, X. Yang, Z. Li, Z. Fang, J. Zhang, C. Zhao, Effects of rhamnolipids on microorganism characteristics and applications in composting: a review, Microbiol. Res. 200 (2017) 33–44.
[24] Y. Liu, X. Ma, G. Zeng, H. Zhong, Z. Liu, Y. Jiang, X. Yuan, X. He, M. Lai, Y. He, Role of low-concentration monorhamnolipid in cell surface hydrophobicity of Pseudomonas aeruginosa: adsorption or lipopolysaccharide content variation, Appl. Microbiol. Biotechnol. 98 (2014) 10231–10241.
[25] X. Mao, R. Jiang, W. Xiao, J. Yu, Use of surfactants for the remediation of contaminated soils: a review, J. Hazard. Mater. 285 (2015) 419–435.
[26] Z. Liu, Z. Zeng, G. Zeng, J. Li, H. Zhong, X. Yuan, Y. Liu, J. Zhang, M. Chen, Y. Liu, G. Xie, Influence of rhamnolipids and triton X-100 on adsorption of phenol by Penicillium simplicissimum, Bioresour. Technol. 110 (2012) 468–473.
[27] Z.F. Liu, G.M. Zeng, J. Wang, H. Zhong, Y. Ding, X.Z. Yuan, Effects of monorhamnolipid and tween 80 on the degradation of phenol by Candida tropicalis, Process Biochem. 45 (2010) 805–809.
[28] R. Thomsen, M.H. Christensen, MolDock: a new technique for high-accuracy molecular docking, J. Med. Chem. 49 (2006) 3315–3321.
[29] Z. Liu, Y. Liu, G. Zeng, B. Shao, M. Chen, Z. Li, Y. Jiang, Y. Liu, Y. Zhang, H. Zhong, Application of molecular docking for the degradation of organic pollutants in the environmental remediation: a review, Chemosphere 203 (2018) 139–150.
[30] K.B. Koziara, M. Stroet, A.K. Malde, A.E. Mark, Testing and validation of the automated topology builder (ATB) version 2.0: prediction of hydration free enthalpies, J. Comput. Aided Mol. Des. 28 (2014) 221–233.
[31] N. Schmid, A.P. Eichenberger, A. Choutko, S. Riniker, M. Winger, A.E. Mark, W.F. van Gunsteren, Definition and testing of the GROMOS force-field versions 54A7 and 54B7, Eur. Biophys. J. 40 (2011) 843–856.
[32] M.J. Abraham, T. Murtola, R. Schulz, S. Páll, J.C. Smith, B. Hess, E. Lindahl, GROMACS: High performance molecular simulations through multi-level parallelism from laptops to supercomputers, SoftwareX 1-2 (2015) 19–25.
[33] J.E. Jones, On the determination of molecular fields. II. From the equation of state of a gas, Proc. R. Soc. Lond. 106 (1924) 463–477.
[34] R. Kumari, R. Kumar, C. Open Source Drug Discovery, A. Lynn, g_mmpbsa–a GROMACS tool for high-throughput MM-PBSA calculations, J. Chem. Inf. Model. 54 (2014) 1951–1962.
[35] B. Kuhn, P.A. Kollman, Binding of a diverse set of ligands to avidin and streptavidin: an accurate quantitative prediction of their relative affinities by a combination of molecular mechanics and continuum solvent models, J. Med. Chem. 43 (2000) 3786–3791.
[36] M. Abdollahi, S. Hassani, M. Derakhshani, Phenol A2 - Wexler, Philip, Encyclopedia of Toxicology, third edition, Academic Press, Oxford, 2014, pp. 871–873.
[37] A. Lebrónpaler, J.E. Pemberton, B.A. Becker, W.H. Otto, C.K. Larive, R.M. Maier, Determination of the acid dissociation constant of the biosurfactant monorhamnolipid in aqueous solution by potentiometric and spectroscopic methods, Anal. Chem. 78 (2006) 7649–7658.
[38] E. Munusamy, C.M. Luft, J.E. Pemberton, S.D. Schwartz, Structural properties of nonionic monorhamnolipid aggregates in water studied by classical molecular dynamics simulations, J. Phys. Chem. B 121 (2017) 5781–5793.
[39] M. Chen, G. Zeng, C. Lai, J. Li, P. Xu, H. Wu, Molecular basis of laccase bound to lignin: insight from comparative studies on the interaction of trametes versicolor laccase with various lignin model compounds, RSC Adv. 5 (2015) 52307–52313.
[40] S.A. Adcock, J.A. McCammon, Molecular dynamics: survey of methods for simulating the activity of proteins, Chem. Rev. 106 (2006) 1589–1615.
[41] H.J.C. Berendsen, J.P.M. Postma, W.F.V. Gunsteren, J. Hermans, Interaction Models for Water in Relation to Protein Hydration, Springer, Netherlands, 1981.
[42] T. Darden, D. York, L. Pedersen, Particle mesh Ewald: an N· log (N) method for Ewald sums in large systems, J. Chem. Phys. 98 (1993) 10089–10092.
[43] R.A. Laskowski, M.B. Swindells, LigPlot+: multiple ligand-protein interaction diagrams for drug discovery, J. Chem. Inf. Model. 51 (2011) 2778–2786.
[44] F. Xu, Oxidation of phenols, anilines, and benzenethiols by fungal laccases: correlation between activity and redox potentials as well as halide inhibition, Biochemistry 35 (1996) 7608–7614.
[45] D. Mo, G. Zeng, X. Yuan, M. Chen, L. Hu, H. Li, H. Wang, P. Xu, C. Lai, J. Wan, C. Zhang, M. Cheng, Molecular docking simulation on the interactions of laccase from trametes versicolor with nonylphenol and octylphenol isomers, Bioprocess. Biosyst. Eng. 41 (2018) 331–343.
[46] K. Holmberg, Interactions between surfactants and hydrolytic enzymes, Colloids Surf. B. Biointerfaces (2017) (in press).
[47] H.M. Lou, M.J. Zeng, Q.Y. Hu, C. Cai, X.L. Lin, X.Q. Qiu, D.J. Yang, Y.X. Pang, Nonionic surfactants enhanced enzymatic hydrolysis of cellulose by reducing cellulase deactivation caused by shear force and air-liquid interface, Bioresour. Technol. 249 (2018) 1–8.
[48] C. Chothia, Hydrophobic bonding and accessible surface area in proteins, Nature 248 (1974) 338.
[49] A. Gutteridge, J.M. Thornton, Understanding nature's catalytic toolkit, Trends Biochem. Sci. 30 (2005) 622–629.
[50] T. Paramo, A. East, D. Garzón, M.B. Ulmschneider, P.J. Bond, Efficient characterization of protein cavities within molecular simulation trajectories:trj_cavity, J. Chem. Theory Comput. 10 (2014) 2151–2164.
[51] M. Chen, G. Zeng, P. Xu, M. Yan, W. Xiong, S. Zhou, Interaction of carbon nanotubes with microbial enzymes: conformational transitions and potential toxicity, Environ. Sci.: Nano 4 (2017) 1954–1960.
[52] X. Peng, X.-z. Yuan, H. Liu, G.-m. Zeng, X.-h. Chen, Degradation of polycyclic aromatic hydrocarbons (PAHs) by laccase in rhamnolipid reversed micellar system, Appl. Biochem. Biotechnol. 176 (2015) 45–55.
[53] D. Chen, N. Oezguen, P. Urvil, C. Ferguson, S.M. Dann, T.C. Savidge, Regulation of protein-ligand binding affinity by hydrogen bond pairing, Sci. Adv. 2 (2016) e1501240.
[54] M. Chen, G. Zeng, C. Lai, C. Zhang, P. Xu, M. Yan, W. Xiong, Interactions of carbon nanotubes and/or graphene with manganese peroxidase during biodegradation of endocrine disruptors and triclosan, Chemosphere 184 (2017) 127–136.
[55] X. Li, Y. Zheng, Lignin-enzyme interaction: mechanism, mitigation approach, modeling, and research prospects, Biotechnol. Adv. 35 (2017) 466–489.
[56] B. Jia, X. Jia, K. Hyun Kim, Z. Ji Pu, M.S. Kang, C. Ok Jeon, Evolutionary, computational, and biochemical studies of the salicylaldehyde dehydrogenases in the naphthalene degradation pathway, Sci. Rep. 7 (2017) 43489.

[57] L. Zhang, Y. Li, Y. Yuan, Y. Jiang, Y. Guo, M. Li, X. Pu, Molecular mechanism of carbon nanotube to activate Subtilisin Carlsberg in polar and non-polar organic media, Sci. Rep. 6 (2016) 36838.
[58] M. Awasthi, N. Jaiswal, S. Singh, V.P. Pandey, U.N. Dwivedi, Molecular docking and dynamics simulation analyses unraveling the differential enzymatic catalysis by plant and fungal laccases with respect to lignin biosynthesis and degradation, J. Biomol. Struct. Dyn. 33 (2015) 1835–1849.
[59] B.A. Noskov, M.M. Krycki, Formation of protein/surfactant adsorption layer as studied by dilational surface rheology, Adv. Colloid Interface Sci. 247 (2017) 81–99.
[60] L. Petridis, R. Schulz, J.C. Smith, Simulation analysis of the temperature dependence of lignin structure and dynamics, J. Am. Chem. Soc. 133 (2011) 20277–20287.
[61] F. Merzel, J.C. Smith, Is the first hydration shell of lysozyme of higher density than bulk water? Proc. Natl. Acad. Sci. U. S. A. 99 (2002) 5378.
[62] D.I. Svergun, S. Richard, M.H. Koch, Z. Sayers, S. Kuprin, G. Zaccai, Protein hydration in solution: experimental observation by x-ray and neutron scattering, Proc. Natl. Acad. Sci. U. S. A. 95 (1998) 2267–2272.
[63] M. Chen, X. Qin, G. Zeng, Single-walled carbon nanotube release affects the microbial enzyme-catalyzed oxidation processes of organic pollutants and lignin model compounds in nature, Chemosphere 163 (2016) 217–226.